Decomposition of perovskite $FeTiO_3$ into wüstite $Fe_{1-x}Ti_{0.5x}O$ and orthorhombic $FeTi_3O_7$ at high pressure

D. Nishio-Hamane,[1,*] T. Yagi,[1] M. Ohshiro,[1] K. Niwa,[2] T. Okada,[1] and Y. Seto[3]
[1]*The Institute for Solid State Physics, The University of Tokyo, Kashiwa 277-8581, Japan*
[2]*Department of Materials Science and Engineering, Nagoya University, Nagoya 464-8603, Japan*
[3]*Department of Earth and Planetary Sciences, Kobe University, Kobe 657-8501, Japan*
(Received 2 June 2010; revised manuscript received 27 July 2010; published 22 September 2010)

The phase relation of $FeTiO_3$ was investigated up to a pressure of about 67 GPa by synchrotron x-ray diffraction and analytical transmission electron microscopy. We found that $FeTiO_3$ perovskite decomposes into $Fe_{1-x}Ti_{0.5x}O$ wüstite and orthorhombic $FeTi_3O_7$ phases (ideally $FeTiO_3 \rightarrow 2/3FeO+1/3FeTi_3O_7$) at conditions above 42 GPa and 2000 K. Our study also demonstrates that the phase assemblage of $Fe_{1-x}Ti_{0.5x}O$ and $FeTi_3O_7$ is the densest of the various systems reported so far for $FeTiO_3$.

DOI: 10.1103/PhysRevB.82.092103 PACS number(s): 61.50.Ks, 62.50.−p, 91.60.Gf

Many ABO_3-type compounds crystallize into the perovskite structure. They represent an important class of materials in physics, materials science, and earth science. Because of this, numerous studies have been conducted to determine the stability and phase transformation sequences of perovskites under extreme conditions. Of the various structures of ABO_3 compounds, the perovskite structure has an extremely high packing efficiency. Consequently, many ABO_3 compounds adopt this structure at very high pressures. Many minerals transform into this structure or an assemblage mainly composed of this structure in the conditions of the earth's deep interior. Silicate perovskite is believed to be the most dominant mineral on our planet. However, the perovskite structure is energetically unfavorable for ABO_3 compounds containing divalent transition metals such as iron, nickel, and cobalt, and most of them decompose into two simple oxides ($ABO_3 \rightarrow AO+BO_2$) at high pressure.[1,2] These transition metals have very limited solubilities in solid solutions, as typified by the $MgSiO_3$-$FeSiO_3$ system. The exception is $FeTiO_3$, which transforms from ilmenite into the perovskite structure at pressures above about 16 GPa;[3] further transformation has been investigated to determine its stability field. After the discovery of the $CaIrO_3$-type postperovskite phase in $MgSiO_3$, many other compounds were found to transform into this postperovskite structure. In addition, first-principles calculations predict that $FeTiO_3$ also adopts this structure at 44 GPa and 0 K, although they predict that its stability region is limited to a relatively narrow pressure range up to 65 GPa.[4] Both theoretical predictions and shock Hugoniot experiments[4,5] suggest that perovskite-type $FeTiO_3$ decomposes into FeO and TiO_2 at pressures above 65 GPa. However, Wu *et al.*[6] performed static high-pressure experiments and reported a completely different result: based on x-ray diffraction (XRD) and Mössbauer measurements, they claim that $FeTiO_3$ perovskite dissociates into $Fe_{1-\delta}Ti_\delta O$ wüstite and $Fe_{1+\delta}Ti_{2-\delta}O_5$ phases at 53 GPa and 2000 K. On the other hand, the decomposed phases were not subjected to chemical analysis in their study, which is indispensable for such an argument.

In the present Brief Report, we report the high-pressure phase behavior of $FeTiO_3$ and conclude that the true reaction is the decomposition of $FeTiO_3$ perovskite into $Fe_{1-x}Ti_{0.5x}O$ and $FeTi_3O_7$, based on high-pressure *in situ* XRD combined with chemical analysis of the recovered sample by analytical transmission electron microscopy (ATEM).

We used a single crystal of $FeTiO_3$ ilmenite that had been carefully synthesized by Takei and Kitamura[7] as the starting material, because commercially available reagent-grade powders often contain some amounts of wüstite, which led to the confusion when we checked the phase relation and the com-

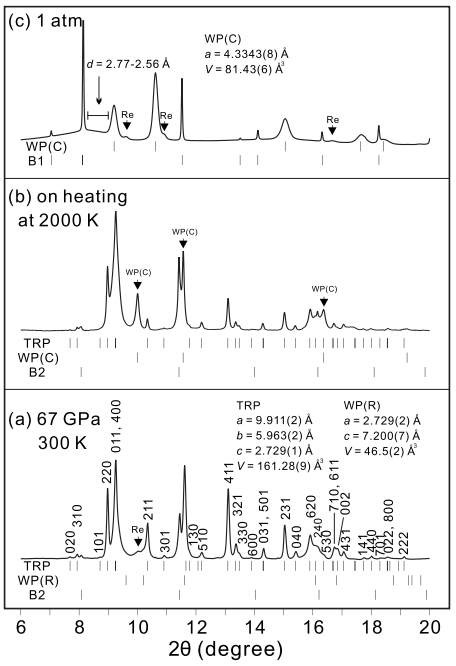

FIG. 1. Representative XRD patterns (wavelength: 0.4001 Å) for $FeTiO_3$. Background was subtracted in each x-ray diffraction pattern. (a) 67 GPa after heating at 2000 K, (b) on heating at 2000 K, and (c) at 1 atm after recovering from 67 GPa. B1: NaCl B1 phase; B2: NaCl B2 phase; Re: rhenium from gasket; TRP: Ti-rich phase ($FeTi_3O_7$, see text); WP(C): cubic wüstite phase; WP(R): rhombohedral wüstite phase. The index for the Ti-rich phase is shown in (a). Bars below x-ray diffraction pattern indicate the peak position calculated on the space group and the determined unit-cell parameters of each phase. The insets give the unit-cell parameters for the space groups of the product phases.

TABLE I. Observed d spacings of the orthorhombic Ti-rich phase ($FeTi_3O_7$, see text) decomposed from $FeTiO_3$ at 67 GPa and 300 K after heating at 2000 K.

$h\ k\ l$	d_{obs} (Å)	$d_{obs}/d_{calc}-1$	I_{obs}
0 2 0	2.9844	0.0009	3.1
3 1 0	2.8916	0.0006	3.8
1 0 1	2.6298	−0.0004	1.3
2 2 0	2.5565	0.0006	71.1
0 1 1[a]	2.4805	−0.0003	100.0
4 0 0[a]	2.4805	0.0011	100.0
2 1 1	2.2188	0.0000	35.6
3 0 1	2.1033	−0.0003	2.9
1 3 0	1.9498	0.0004	7.3
5 1 0	1.8825	0.0008	5.9
4 1 1	1.7530	−0.0002	70.9
3 2 1	1.7185	−0.0003	14.7
3 3 0	1.7043	0.0006	5.5
6 0 0	1.6517	−0.0001	1.0
0 3 1[a]	1.6048	−0.0012	10.2
5 0 1[a]	1.6048	−0.0007	10.2
2 3 1	1.5285	0.0001	34.0
0 4 0	1.4907	−0.0001	7.4
6 2 0	1.4449	0.0000	24.3
2 4 0	1.4283	0.0005	13.8
5 2 1	1.4128	0.0003	7.2
5 3 0	1.4040	0.0003	5.0
6 1 1	1.3742	−0.0006	13.5
0 0 2	1.3661	0.0013	12.3
4 3 1	1.3490	0.0007	9.2
1 4 1	1.2957	−0.001	2.2
4 4 0	1.2777	0.0002	3.8
7 0 1	1.2546	−0.0017	2.1
0 2 2[a]	1.2399	−0.0006	3.0
8 0 0[a]	1.2399	0.0008	3.0
2 2 2	1.2039	0.0003	3.3

[a]Peak overlap. a=9.911(2) Å, b=5.963(2) Å, c=2.729(1) Å, and V=161.28(9) Å^3.

positions after experiment. The single crystal was crushed and powdered using a mortar and pestle and formed into a pellet. It was then sandwiched between NaCl pellets and loaded into the sample chamber. High pressures were generated using a lever-type diamond-anvil cell. Heating was conducted using two focused fiber lasers with a beam size of 10–20 μm in diameter from two sides and the sample was scanned by the laser during heating. The pressure was determined from the unit-cell volumes of NaCl (Ref. 8) and the Raman shift of the diamond anvil.[9] Angle-dispersive XRD measurements were conducted at high pressure using the BL13A beamline at the Photon Factory of KEK and the BL10XU beamline at SPring-8. These beam lines provide a collimated beam (15–30 μm in diameter) of monochromatic x-ray radiation (wavelength: 0.4001–0.4266 Å). The

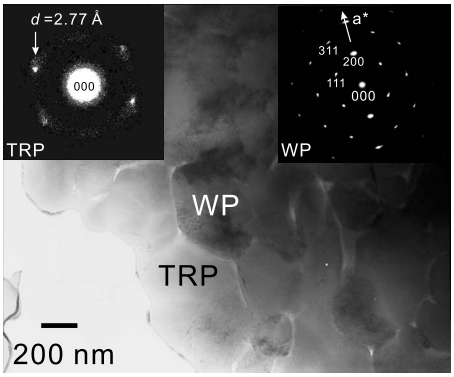

FIG. 2. Representative bright-field image and selected-area diffraction patterns of the recovered sample for $FeTiO_3$ from 65 GPa after heating at 2000 K. TRP: Ti-rich phase ($FeTi_3O_7$, see text); WP: wüstite phase. TRP and WP appear as low and high contrasts in the bright-field image, respectively, depending on their crystalline state.

analysis of the x-ray diffraction pattern was done in each peak. All x-ray diffraction peaks were fitted by the Marquardt algorithm (the nonlinear least-squares method) using the symmetric pseudo-Voigt function as a fitting function. The symmetry and the Miller indices of the unknown phase were investigated by the Monte Carlo method using the PDINDEXER software.[10] The detail of the fitting and indexing algorithm is described in Seto *et al.*[10] The recovered sample was also observed by ATEM (JEM-2010F; JEOL) using a voltage of 200 kV and an energy-dispersive system (EDS) at the Institute for Solid State Physics of the University of Tokyo. Quantitative chemical analysis was performed using the experimentally obtained k factors of Fe/Ti ratio using $FeTiO_3$ ilmenite as standard, which are correction factors for ATEM-EDS analysis.[11]

X-ray diffraction measurements were performed at high pressures. A single phase of $FeTiO_3$ perovskite was observed up to 38 GPa, whereas the diffraction pattern changed at pressures above 42 GPa after heating. Figure 1 shows representative XRD patterns after this change. Our diffraction patterns are almost identical with those obtained by Wu *et al.*[6] Our XRD patterns contain diffraction lines for the wüstite

TABLE II. Chemical compositions of the Ti-rich ($FeTi_3O_7$, see text) and wüstite phases in the sample recovered from 65 GPa after heating at 2000 K.

	$FeTi_3O_7$ phase (wt %)	Wüstite (wt %)
TiO_2	77.5(30)	5.1(6)
FeO	22.5(15)	94.9(30)
Total	100	100
	Cation (O=7)	Cation (O=1)
Ti	3.01	0.04
Fe	0.97	0.91
Total	3.98	0.95

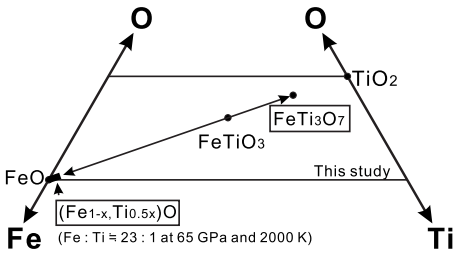

FIG. 3. Phase relation for $FeTiO_3$ at high pressures above 40 GPa and high temperatures in Fe-Ti-O ternary system. As wüstite contains 4 mol % Ti at 65 GPa, the phase ratio $Fe_{1-x}Ti_{0.5x}O$ wüstite:$FeTi_3O_7$ phase is calculated to be about 2.21:0.97.

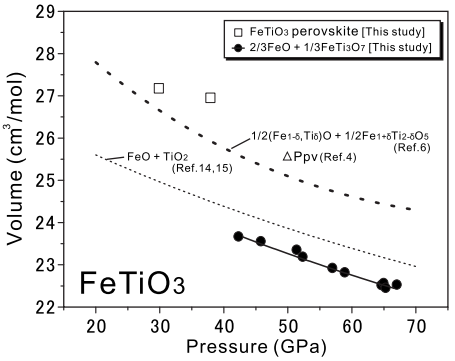

FIG. 4. Pressure dependence of volumes of the high-pressure phase assemblages in $FeTiO_3$ system at 300 K. The decomposition assemblage of $Fe_{1-x}Ti_{0.5x}O$ and $FeTi_3O_7$ in this study was calculated to be ideally $3/2FeO+1/3FeTi_3O_7$, although a little Ti was incorporated into the wüstite phase. Second-order Birch-Murnaghan equation of state fitting yields $K_0=141(20)$ and 281(28) GPa on $V_0=12.3(3)$ and 57.6(7) cm^3/mol for the wüstite and $FeTi_3O_7$ phases, respectively.

phase, which implies that $FeTiO_3$ perovskite dissociates into wüstite (a Fe-rich phase) and a Ti-rich phase. However, as shown in Table I, the diffraction lines for the Ti-rich phase can be better explained by an orthorhombic symmetry than the $C2/c$ symmetry proposed by Wu *et al.*[6] The unit-cell parameters for the Ti-rich phase were $a=9.911(2)$ Å, $b=5.963(2)$ Å, $c=2.729(1)$ Å, and $V=161.28(9)$ Å^3 at 67 GPa, and the possible space groups are $I222$ ($I2_12_12_1$), $Imm2$, and $Immm$. The diffraction pattern of the recovered sample has a very broad, weak peak around $d=2.77-2.56$ Å together with peaks for the wüstite phase, which reverted to cubic symmetry (Fig. 1). The unit-cell parameter of the recovered wüstite was $a=4.3343(8)$ Å, which is indistinguishable from that of pure FeO wüstite ($a=4.334$ Å),[12] although it contains a small amount of Ti (see discussion below).

The sample recovered from 65 GPa after heating at 2000 K was investigated by ATEM. Figure 2 shows a bright-field image and selected-area electron-diffraction patterns. They clearly reveal a two-phase assemblage of wüstite and the Ti-rich phase. The Ti-rich phase shows only very weak electron reflections at around $d=2.77$ Å with a broad peak on the low-d side, whereas the electron diffractions of wüstite can be indexed as $Fm\bar{3}m$ (Fig. 2). These results are in good agreement with the XRD measurements. Table II lists representative chemical compositions of the Ti-rich phase and wüstite. It is clear that the Ti/Fe ratio of the Ti-rich phase is about 3 and the composition of the Ti-rich phase can be defined as $FeTi_3O_7$, rather than $Fe_{1+\delta}Ti_{2-\delta}O_5$ proposed by Wu *et al.*,[6] although they have similar XRD patterns. Wüstite also contained a minor component of Ti.

Figure 3 summarizes the high-pressure phase relation of $FeTiO_3$ above 42 GPa. In the present study, $FeTiO_3$ decomposed into an assemblage of wüstite and the $FeTi_3O_7$ phase above 42 GPa, ideally $FeTiO_3 \rightarrow 2/3FeO+1/3FeTi_3O_7$, although wüstite contains small amounts of Ti (Table II). Since the $FeTi_3O_7$ composition lies on the FeO-TiO_2 tie line, the impure wüstite composition can be described as $Fe_{1-x}Ti_{0.5x}O$ when the redox state is preserved from the starting material (Fig. 3). In the wüstite structure, the minor amount of TiO_2 in the $Fe_{1-x}Ti_{0.5x}O$ composition may result cation defects as observed in Ti-doped MgO.[13] The unit-cell parameter of the recovered wüstite was indistinguishable from that of pure FeO wüstite, although the structure should include the cation defects. However, the effect of TiO_2 incorporation on the unit-cell parameters of the wüstite structure has not been established yet even under ambient pressure. Precise measurements of the unit-cell parameter of the wüstite phase on FeO-TiO_2 system under high pressure and on recovered sample will be necessary to better elucidate the incorporation of the TiO_2.

We attempted to solve the crystal structure of the $FeTi_3O_7$ phase using all the XRD data obtained in the present study and data for compounds with similar stoichiometries and symmetries but so far the structure model remains unclear. However, since the two-phase assemblage of $Fe_{1-x}Ti_{0.5x}O$ wüstite and the $FeTi_3O_7$ phase must be denser than the perovskite phase, the Z number of the $FeTi_3O_7$ phase should be 2 in the orthorhombic unit cell. Figure 4 shows the molar volume for the phases in the $FeTiO_3$ system. As shown in Fig. 4, the phase assemblage of $Fe_{1-x}Ti_{0.5x}O$ and $FeTi_3O_7$ is the densest of all the $FeTiO_3$ system that have been reported.[14,15] Its density increases by about 10% when $FeTiO_3$ perovskite decomposes into the $Fe_{1-x}Ti_{0.5x}O$ and $FeTi_3O_7$ assemblage at about 40 GPa. Transitions from perovskite into the $CaIrO_3$-type postperovskite phase generally result in density increase of just a few percent; thus, it is interesting that the present decomposition results in a much larger density increase. Various transition sequences have been reported for the high-pressure behavior of perovskite-type compounds but so far no decomposition into $AO+AB_3O_7$ type compounds has been reported. Structural analysis of the recently found $FeTi_3O_7$ is highly desirable to understand the peculiar behavior of $FeTiO_3$ at high pressures.

High-pressure *in situ* x-ray experiments were conducted at the Photon Factory and SPring-8 under the auspices of Proposals No. 08G042 and No. 2009B1238, respectively. We are grateful for the technical support for ATEM by M. Ichihara at ISSP of the University of Tokyo. D.N-H. is supported by the Japan Society for the Promotion of Science.

*Corresponding author; hamane@issp.u-tokyo.ac.jp

[1] E. Ito, Phys. Earth Planet. Inter. **10**, 88 (1975).
[2] E. Ito and M. Matsui, Phys. Chem. Miner. **4**, 265 (1979).
[3] K. Leinenweber, W. Utsumi, Y. Tsuchida, T. Yagi, and K. Kurita, Phys. Chem. Miner. **18**, 244 (1991).
[4] N. C. Wilson, S. P. Russo, J. Muscat, and N. M. Harrison, Phys. Rev. B **72**, 024110 (2005).
[5] L. Liu, Phys. Earth Planet. Inter. **10**, 167 (1975).
[6] X. Wu, G. Steinle-Neumann, O. Narygina, I. Kantor, C. McCammon, V. Prakapenka, V. Swamy, and L. Dubrovinsky, Phys. Rev. Lett. **103**, 065503 (2009).
[7] H. Takei and K. Kitamura, J. Cryst. Growth **44**, 629 (1978).
[8] N. Sata, G. Shen, M. L. Rivers, and S. R. Sutton, Phys. Rev. B **65**, 104114 (2002).
[9] Y. Akahama and H. Kawamura, J. Appl. Phys. **96**, 3748 (2004).
[10] Y. Seto, D. Nishio-Hamane, T. Nagai, and N. Sata, Rev. High Pressure Sci. Technol. **20**, 269 (2010).
[11] G. Cliff and G. W. Lorimer, J. Microsc. **103**, 203 (1975).
[12] C. A. McCammon and L. Liu, Phys. Chem. Miner. **10**, 106 (1984).
[13] K. C. Yang and P. Shen, J. Solid State Chem. **178**, 661 (2005).
[14] D. Nishio-Hamane, A. Shimizu, R. Nakahira, K. Niwa, A. Sano-Furukawa, T. Okada, T. Yagi, and T. Kikegawa, Phys. Chem. Miner. **37**, 129 (2010).
[15] S. D. Jacobsen, J. Lin, R. J. Angel, G. Shen, V. B. Prakapenka, P. Dera, H. Mao, and R. J. Hemley, J. Synchrotron Radiat. **12**, 577 (2005).